UDK 528.9:528.7(55)
Review / Pregledni znanstveni članak

Investigating Playa Patterns in Isfahan Province via Remote Sensing Techniques

Zahra MESMARIAN – Tehran[1]

ABSTRACT. Playas are crucial water storage and recharge areas in a predominantly arid and semiarid climate. Mapping playas helps determine their locations, sizes, and hydrological characteristics, providing valuable information for assessing water availability, planning for sustainable water use, and understanding the role of playas in groundwater recharge. Since comprehensive research on identifying all playas in Isfahan Province has not been conducted, presenting a suitable method for their detection can be a significant step in understanding, utilizing, and preserving these areas. Employing remote sensing as an efficient, fast, and highly accurate solution can effectively identify these phenomena. In this regard, Landsat satellite images spanning different months throughout 2023 were gathered for Isfahan Province. Integrating various spectral indices, such as NDWI, SWI, and AWEI for water detection and NDSI for saline areas, significantly enhances the precision of playa delineation. After the application of filters and spectral indices to Landsat satellite images, a total of 24 playas were identified within Isfahan province. Notably, Isfahan and Nain counties had the highest numbers of playas, with 9 and 7 playas, respectively. Among the identified playas, the most significant area was observed in Khur, covering approximately 2250 square kilometers, with a significant portion of its surface covered by salt crust, reaching up to 1300 square kilometers. In order to validate the accuracy of the results, a precise process involving the collection of 106 ground truth points through GPS measurements was conducted. This validation confirms the accuracy of boundary delineation, underscoring the efficacy of remote sensing and GIS technologies in this context.

Keywords: arid regions, Geographic Information Systems (GIS), Isfahan Province, playa mapping, remote sensing, spectral indices.

[1] Zahra Mesmarian, corresponding author, Department of Irrigation and Drainage Engineering, Aburaihan Campus, University of Tehran, Tehran, Iran, e-mail: mesmarian.zar@gmail.com

1. Introduction

Flat landforms, known as playas, are crucial water storage and recharge areas primarily found in interior desert basins and adjacent coastal areas characterized by semiarid and arid climates. These areas have slopes of less than 0.02% (Mirzadeh et al. 2023). Playas typically form in closed basin environments, where there is no outlet for water drainage, and they are recharged directly from precipitation and runoff (Haukos and Smith 1994).

Playas are characterized by their periodic water presence. They often remain dry for extended periods but may temporarily fill with water during rainfall events or through groundwater discharge. This cyclical water availability contributes to playas' unique ecological adaptations and processes (Mitsch et al. 2009). The sediments found within playas are diverse and can vary depending on the geological characteristics of the surrounding area. The composition of the sediment influences the fertility of playas and their ability to support vegetation and wildlife. As the water in Playas evaporates, it leaves behind concentrated salts and minerals on the surface, forming salt flats and evaporate deposits (Mirzadeh et al. 2023).

Landform mapping typically involves a combination of field observation, pre-prepared maps, and collected data from various sources. However, this approach often leads to outdated, limited, and imprecise information due to differences in the spatial and temporal resolutions of the data (Dixon 1998, Embabi and Moawad 2014). Field observations provide detailed but time-consuming and limited coverage. Existing maps may not specifically focus on the landforms being mapped, and data sources can vary in quality and accuracy. Advanced mapping techniques like remote sensing and GIS are being utilized to improve accuracy and currency (Adam et al. 2010, Lang et al. 2015, Lyon et al. 2001, Ozesmi and Bauer 2002, Rebelo et al. 2008, Sader et al. 1995).

In this regard, Schneevoigt and Schrott (2006); showed that alpine landforms could be detected using a multiscale and hierarchical classification derived from ASTER imagery and DEM. Wu (2018); implemented cutting-edge, high-resolution light detection and ranging (LiDAR) data and aerial imagery to comprehensively assess wetland mapping and monitoring. Bowen et al. (2010); established a comprehensive Geographic Information Systems (GIS) database to identify and map 22,045 ephemeral playa wetlands in the High Plains, particularly in Kansas, surpassing previous estimates. Smith et al. (2011); compared visualization techniques for Digital Elevation Models (DEMs) in landform mapping. No single method offers a complete and unbiased representation. However, curvature visualization is recommended for initial mapping, supplemented by relief-shaded visualizations. Kaplan and Avdan (2017); effectively applied Sentinel-2 remote sensing techniques, incorporating various classification methods and using the Normalized Difference Vegetation Index (NDVI) and Normalized Difference Water Index (NDWI) to classify wetland contents, resulting in a notable kappa coefficient of 0.95, highlighting the efficacy of their approach. In the study conducted by Mui et al. (2015); a multiscale Geographic Object-Based Image Analysis (GEOBIA) approach was used to accurately map wetlands in diverse landscapes, including areas influenced by human activi-

ties. Integrating the normalized-difference vegetation index (NDVI) enhanced wetland delineation accuracy. Halabisky et al. (2022) addressed the challenge of incomplete wetland inventories by developing the Wetland Intrinsic Potential (WIP) tool. This tool employs a novel approach, combining hydrophytic vegetation, hydrology, hydric soil indicators, and multiscale topographic data to create a spatially explicit wetland probability map.

Since comprehensive research on identifying all playas in Isfahan Province has not been conducted to date, presenting a suitable method for their detection can be a significant step in understanding, utilizing, and preserving these areas.

Employing remote sensing satellite systems with different spatial resolutions and repeat cycles, accompanied by the recent technological improvements in remote sensing and surveying methods, can be an effective technique for identifying playas, particularly in dry and semi-arid regions where numerous playas exist (Slaymaker 2001, Hammond 1964).

In this study, to enhance the accuracy of mapping playa borders, we integrated various spectral indices, including the Normalized Difference Water Index (NDWI), Soil Water Index (SWI), Automated Water Extraction Index (AWEI), and Normalized Difference Salinity Index (NDSI). These indices were selected for their ability to detect water bodies and saline areas, which are critical playas features. By applying filters and indices to Landsat satellite images, 24 playas were identified in Isfahan Province.

2. Materials and Methods

2.1. Study Area

Isfahan province, situated in the central region of Iran, spans an area of approximately 107 square kilometers, with geographical coordinates ranging between 30 to 34 degrees north latitude and 49 to 55 degrees east longitude. The province comprises 28 counties, delineated by red borders on the map. Notably, Khur, Naein, Ardestan, and Isfahan emerge as the most prominent counties within Isfahan province (Fig. 1). Characterized by an average annual 14 degrees Celsius, the province falls within the climatic classification of a warm and arid temperature approximately region precipitation of around 220 millimeters and an average annual temperature of approximately 14 degrees Celsius, the province falls within the climatic classification of a warm and arid region.

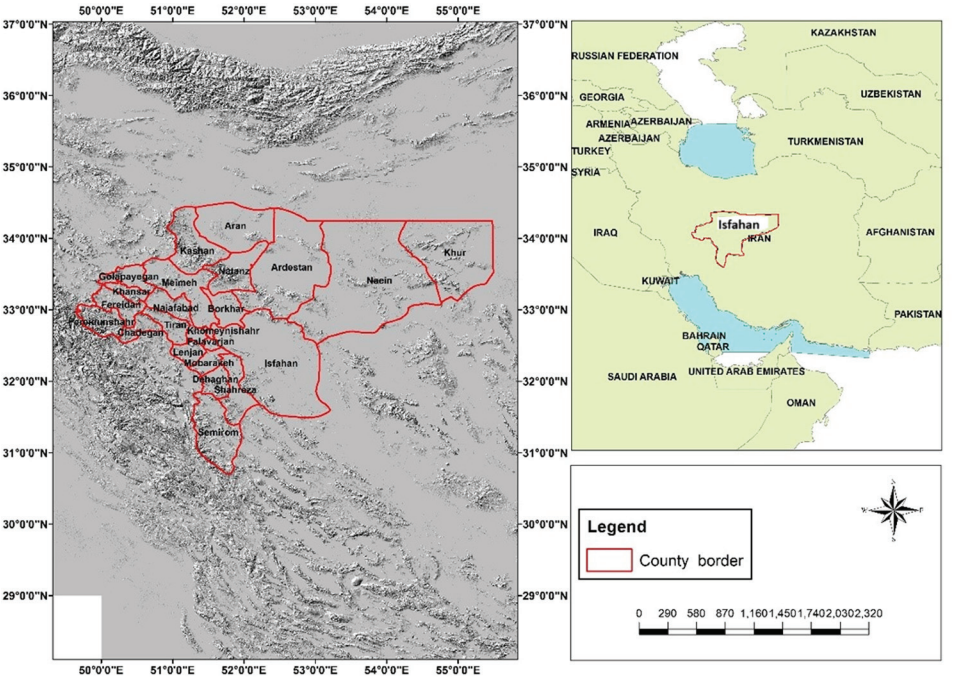

Fig. 1. *Geography of Isfahan.*

2.2. Satellite Data

Landsat-8, owned and operated by NASA and the USGS, offers globally georeferenced images and image processing capabilities. It has two main instruments: the Operational Land Imager (OLI) and the Thermal Infrared Sensor (TIRS) (Acharya and Yang 2015).

The OLI is a push-broom sensor with a four-mirror telescope specifically designed to capture data in the visible, near-infrared, and shortwave infrared wavelengths, including a panchromatic band Acharya and Yang (2015); Meanwhile, TIRS collects data using two long-wavelength thermal infrared bands. The TIRS data has a spatial resolution of 100 meters and is carefully aligned with the OLI data to generate radiometrically and geometrically calibrated, terrain-corrected 16-bit Level 1 data products (Acharya and Yang 2015). These instruments support various applications, including cartography, land use analysis, forestry management, coastal zone monitoring, and flood risk management (Miller 2016).

Bands 1 to 7 of Landsat-8 offer a spatial resolution of 30 meters, Band 8 has a spatial resolution of 15 meters, and Band 9 has a spatial resolution of 30 meters. Bands 10 and 11 are thermal infrared bands (TIR) that record the

temperature of the Earth's surface and objects. They have a spatial resolution of 100 meters. The TM sensor on this satellite collects data from three visible bands (red, green, and blue), one near-infrared band, two mid-infrared bands, and one thermal infrared band, making a total of seven bands (Table 1).

Table 1. *Summary of Landsat 8 Spectral Bands and Characteristics (U.S. Geological Survey, URL 1).*

Band	Name	Wavelength (Micrometers)	Spatial Resolution (meters)
Band 1	Coastal aerial	0.43–0.45	30
Band 2	Blue	0.45–0.51	30
Band 3	Green	0.53–0.59	30
Band 4	Red	0.64–0.67	30
Band 5	Near Infrared (NIR)	0.85–0.88	30
Band 6	Shortwave Infrared 1 (SWIR1)	1.57–1.65	30
Band 7	Shortwave Infrared 2 (SWIR2)	2.11–2.29	30
Band 8	Panchromatic	0.50–0.68	15
Band 9	Cirrus	1.36–1.38	30
Band 10	Longwave Infrared 1 (LWIR1)	10.6–11.19	100
Band 11	Longwave Infrared 2 (LWIR2)	11.50–12.51	100

2.3. Spectral indices

To delineate the boundaries of playas, the combination of the spectral indices including the Normalized Difference Water Index (NDWI), Soil Wetness Index (SWI), Automated Water Extraction Index (AWEI), and Normalized Differential Salinity Index (NDSI) were utilized. While a threshold of 0 was initially applied to each index map during the surface water extraction process, it has been noted in previous studies that this threshold may not always yield optimal extraction performance across all areas (Xu 2006, Guo et al. 2017). Therefore, to achieve the highest overall accuracy, an optimal threshold was determined using the Otsu threshold method (Xu et al. 2011). By integrating these indices, we can enhance the accuracy and reliability of playa delineation. The combined approach allows us to account for the diverse characteristics of playas and improve our ability to identify these features in remote sensing imagery. Ultimately, using a combination of spectral indices increases the robustness of our analysis and enables a more comprehensive assessment of playa environments.

2.3.1. Normalized Difference Water Index (NDWI)

Normalized Difference Water Index (NDWI): This index is valuable for distinguishing between land and water due to water surfaces' strong electromagnetic radiation absorption, resulting in low reflectance. Playas often contain ephemeral or seasonal water bodies, and NDWI can effectively identify these features by comparing the reflectance in the near-infrared (NIR) and GREEN spectral bands. NDWI ranges from –1 to 1, where values near 1 indicate water bodies or high humidity, and values near –1 represent dry areas or lack of moisture (Gao 1996). NDWI is calculated using (1):

$$NDWI = \frac{GREEN - NIR}{GREEN + NIR}. \tag{1}$$

2.3.2. Soil Wetness Index (SWI)

SWI is a crucial agricultural, hydrology, and environmental science indicator to assess soil moisture levels (Gasmi et al. 2022). According to (2), it combines data from various spectral bands to provide a comprehensive soil wetness index. Positive SWI values indicate wetter soil conditions, while negative values suggest drier soil. SWI values range from –1 to 1, with values near 1 indicating water-saturated or highly humid soil and near –1 representing arid or moisture-deprived regions.

$$\begin{aligned} SWI = {} & (Blue \cdot 0.2626) + (Green \cdot 0.2141) + (Red \cdot 0.0926) + (NIR \cdot (-0.0656)) + \\ & + (SWIR1 \cdot (-0.7629)) + (SWIR2 \cdot (-0.5388)) \end{aligned} \tag{2}$$

2.3.3. Automated water extraction index (AWEI)

AWEI is another indice designed specifically for extracting water bodies from satellite imagery, making it a valuable tool for delineating playas. AWEI enhances our ability to detect water bodies within playas, even in challenging environmental conditions or under different illumination angles. This index incorporates a thresholding technique to identify water pixels, taking into account factors such as shadowing and land cover variability (Feyisa et al. 2014). The AWEI comprises two indices: AWEInsh, applied in scenarios without shadows, and AWEIsh, designed for distinguishing water pixels from shadow pixels. Numerous recent studies, such as the work conducted by Tulbure et al. (2016); have employed the AWEI for the purpose to delineate water bodies in Landsat imagery.

2.3.4 Normalized differential salinity index (NDSI)

Certain regions, particularly those with clay and salt deposits such as playas, require specialized indices for accurate identification. Specifically, for clay-rich areas, which exhibit high reflectance in band 5 and low reflectance in band 7, the ratio of band 5 to 7 proves effective in identifying these clay zones.

In a study by Khan (2002); various combinations of spectral reflectance for salt-affected soils were tested. However, it was noted that the primary indices proposed by Khan and Sato (2001); demonstrated superior performance in the identification of saline areas and the reduction of areas with dense vegetation (3), (4), (5).

$$NDSI = \frac{GREEN - RED}{GREEN + RED} \tag{3}$$

$$SI_1 = \sqrt{BLUE \cdot GREEN} \tag{4}$$

$$SI_2 = \sqrt{BLUE^2 + GREEN^2} \tag{5}$$

2.4. Satellite Image Extraction Method

To delineate the boundaries of the plains in Isfahan province, Landsat 8 satellite images for rows and paths 37-162, 37-163, 38-163, 164-36, 164-37, and 37-165 were collected from the U.S. Geological Survey's Landsat Archives (Fig. 2). These images underwent preprocessing, which included atmospheric and geometric correction and image mosaic creation, to ensure accurate and seamless data integration for subsequent analysis. While the images were acquired simultaneously to ensure comprehensive coverage, they provide a snapshot of the diverse land features and landscapes across Isfahan Province. This dataset encompasses various topographic and land cover characteristics, which, when analyzed, allow us to infer information about the region's general climate patterns, including potential variations between dry and wet seasons.

Subsequently, water indices (NDWI, SWI, AWEI) were implemented to detect water regions, facilitating the distinction between artificial lakes, such as dams, lakes, reservoirs behind dams, flood-spreading zones, recreational lakes, and natural lakes. In the final step, the salinity-sensitive index (NDSI) was applied to the isolated natural water regions to emphasize playas' distinctive clay-based and salt-crust bottom characteristics.

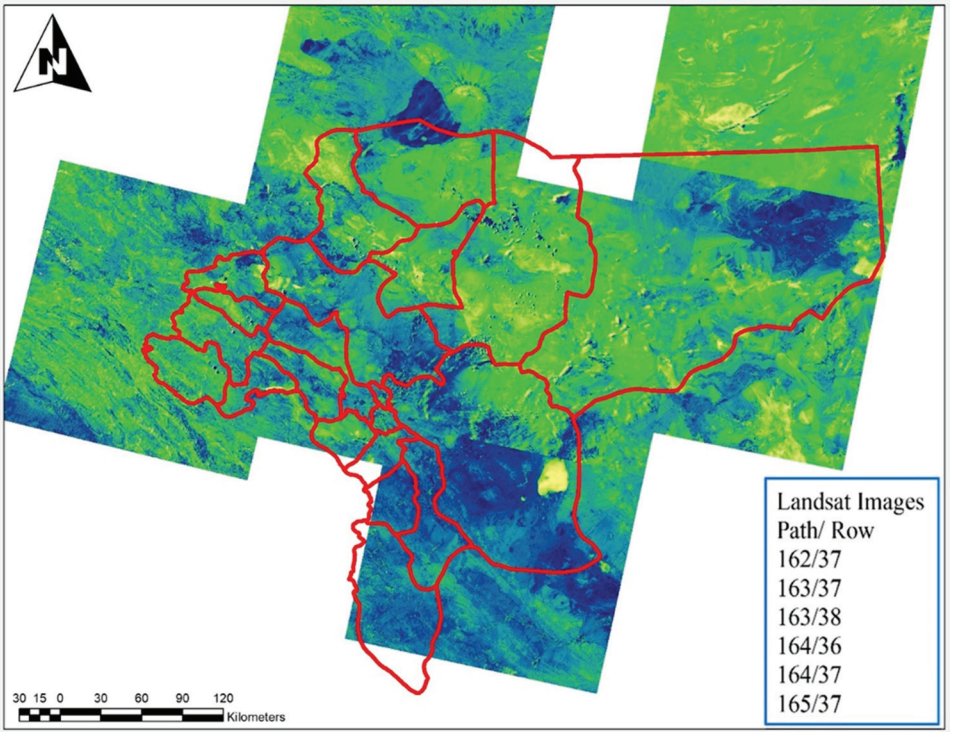

Fig. 2. *Satellite images used for the study area.*

3. Results and Discussion

3.1. Performance Comparison of Water Indices

This study conducted a comprehensive evaluation of the Normalized Difference Water Index (NDWI), Soil Wetness Index (SWI), and Atmospherically Resistant Vegetation Index (AWEI) to assess their effectiveness in extracting surface water from Landsat data. Alongside the salinity index, the Normalized Differential Salinity Index (NDSI) is used in mapping playas within Isfahan province.

According to Table 2, results from the evaluation revealed that AWEI consistently outperforms NDWI and SWI in both Overall Accuracy and Kappa Coefficient. AWEI's higher accuracy metrics (Overall Accuracy: 0.93, Kappa Coefficient: 0.84) suggest its superior efficacy in accurately delineating water bodies within playas. Additionally, NDSI exhibits high Overall Accuracy (0.90)

and Kappa Coefficient (0.86) values, indicating its effectiveness in identifying saline areas within playas. This result underscores the utility of NDSI for characterizing the unique geological composition of playas and highlights its complementary role alongside the water extraction indices.

Table 2. *Accuracy Metrics for Water Extraction and Salinity Indices.*

Indices	Overall Accuracy	Kappa Coefficient (k)
NDWI	0.88	0.72
SWI	0.89	0.73
AWEI	0.93	0.84
NDSI	0.90	0.86

3.2. Validation and Ground Truth Data

In order to ensure the accuracy of the identified playa boundaries, a validation process was conducted. While the initial boundaries were determined based on satellite imagery from Landsat8, it was essential to cross-verify and refine these boundaries using ground truth data obtained through GPS measurements. A total of 106 ground truth points were collected for this purpose, as depicted in Fig. 3.

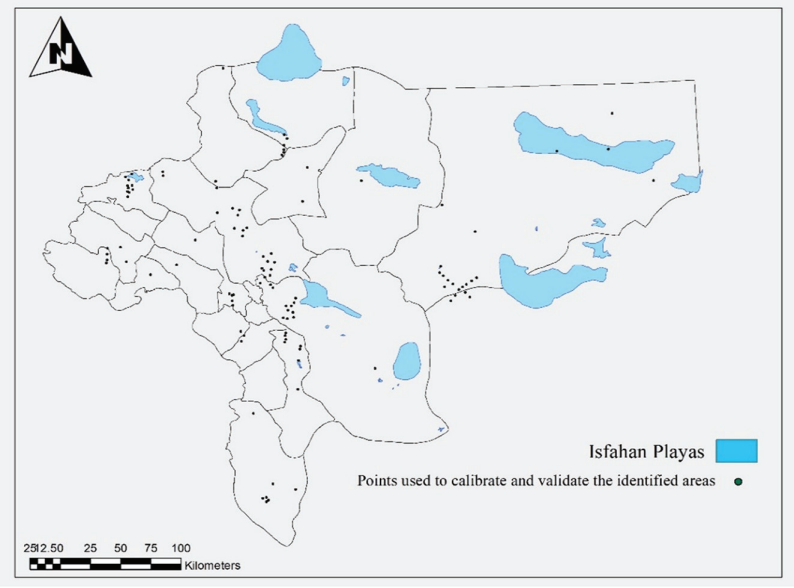

Fig. 3. *Ground truth points used for validation and refinement of identified playa boundaries.*

These ground truth points were critical in validating and fine-tuning the playa boundaries. Any discrepancies or inaccuracies in the initial boundaries were identified and corrected by comparing the boundaries delineated through satellite imagery with the precise GPS measurements. The validation indicates that the delineation of playa boundaries was good because it demonstrated a close alignment between the satellite-derived boundaries and the ground truth data, ensuring a high level of reliability in the delineation process.

3.3. Geographic Distribution of Identified Playas

Fig. 4 and Table 3 illustrate the boundaries of the 24 identified playas in Isfahan province, categorized by counties and areas. These playas are spread across various towns, demonstrating their diverse regional presence.

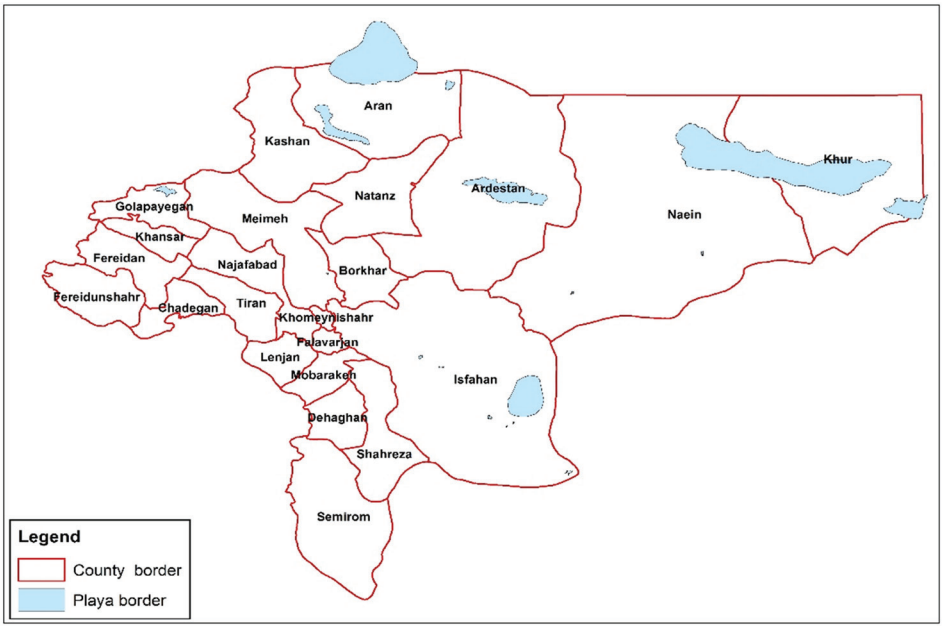

Fig. 4. *Identified Playa's boundary location in Isfahan province.*

Table 3. *Playa's boundary in Isfahan province by counties and areas.*

Number	Playa's Name	Counties	Area (km^2)	Number	Playa's Name	Counties	Area (km^2)
1	Ardestan	Ardestan	450	13	Siyah Kooh	Nain	500
2	Aran 1	Aran-Bidgol	320	14	Biadeh	Nain	267
3	Aran 2	Aran-Bidgol	28.8	15	Rig Zarin 1	Nain	159
4	Gavkhuni Playa	Isfahan	550	16	Rig Zarin 2	Nain	45
5	Gavkhuni Playa 1	Isfahan	4.9	17	Khur-Chupanan	Nain	2250
6	Gavkhuni Playa 2	Isfahan	0.115	18	Bafran	Nain	2.15
7	Gavkhuni Playa 3	Isfahan	0.383	19	Anarak	Nain	3.18
8	Gavkhuni Playa 4	Isfahan	0.82	20	Lake Namak	Aran-Bidgol	1600
9	Segzi	Isfahan	300	21	Shahreza	Shahreza	8.6
10	Mohammadabad 1	Isfahan	4.5	22	Golpayegan	Golpayegan	48
11	Mohammadabad 2	Isfahan	2.16	23	Mimeh	Mimeh	23
12	Hasanabad	Isfahan	4.5	24	Morcheh Khort	Mimeh	0.82

3.4. Size and Economic Potential

Isfahan and Nain counties are particularly notable for their high concentration of playas, with 9 and 7 playas, respectively. Among these identified playas, the largest one is "Khur-Chupanan", which spans approximately 2250 square kilometers and features a salt crust extending over an area of up to 1300 square kilometers. This playa is among the 60 identified playas in Iran and is renowned for its high potassium content. The Khur-Tabs road intersects it. Other significant playas, such as "Gavkhuni Playa", "Namak Playa", "Ardestan Playa" and "Siakouh Playa", have respective areas of 550, 1600, 450, and 500 square kilometers. Despite their considerable economic and potential tourist value, these playas have been underutilized due to their relatively unknown status.

3.5. Gavkhuni Playa

The identified salt flats in Isfahan Province, specifically the Gavkhuni Playa, stand out as the most renowned in the region. The sole salt playa in Isfahan served as a habitat for diverse plant and animal species during wet years. Situated at the entrance of the Varzaneh Desert in the southeast of Isfahan, this playa covers an estimated area of 550 square kilometers, as determined by spectral indices in this study.

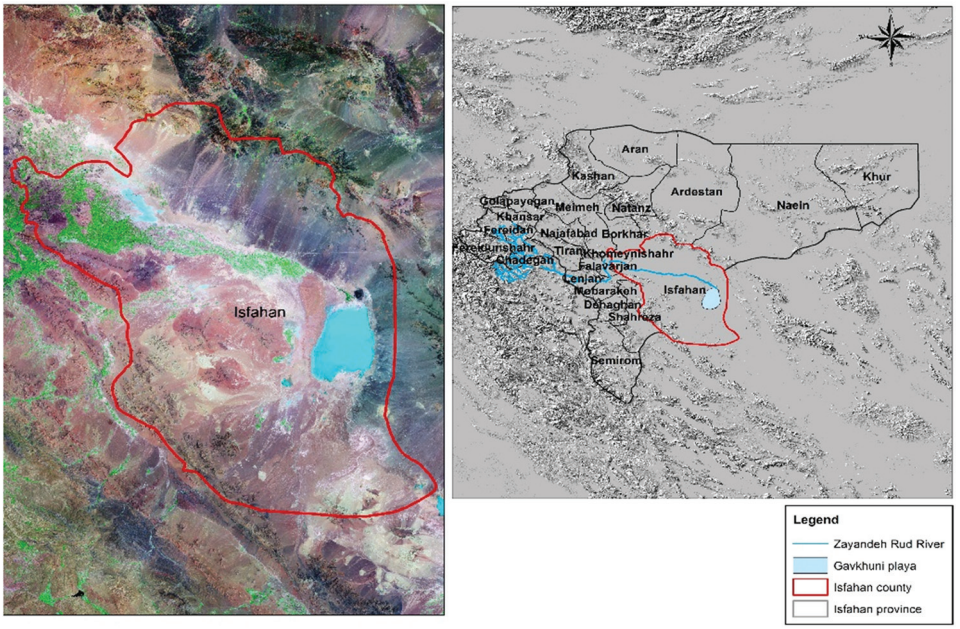

Fig. 5. *The geographical location of Gavkhuni Wetland in Isfahan Province.*

The primary recharging source of the Gavkhuni Playa is the Zayandeh Rud River.

Originating from the Zagros Mountains in the Bakhtiari region in the western part of the province, the Zayandeh Rud River, instead of flowing into the sea and continuing its natural course, diverts towards the Gavkhuni Playa at the entrance of the Varzaneh Desert in the southeast of Isfahan, where it comes to a halt. Due to recent years' droughts and a significant decrease in the river's water supply, the inflow of water into the GavkhuniSalt Playa has sharply declined. This reduction has led to the extinction of plant and animal species within the playa, transforming it into a primary center for airborne dust particles in Isfahan Province.

Fig. 5 illustrates the geographical location of the Gavkhuni Playa in Isfahan Province and Fig. 6 and Fig. 7 depict the Zayandeh Rud River's path towards the Gavkhuni Salt Playa, the initial section of the playa, and the saline and salt flat areas within it.

Fig. 6. *Zayandeh Rud River, the main recharging source of Gavkhuni Playa.*

Fig. 7. *The beginning section of Gavkhuni Playa.*

4. Conclusion

This study delved into the intricate landscape of Isfahan province, Iran, employing a multifaceted approach combining satellite imagery analysis, spectral indices, and ground truth validation to identify and characterize playas within the region. Through the utilization of advanced techniques such as the Normalized Difference Water Index (NDWI), Soil Wetness Index (SWI), Automated Water Extraction Index (AWEI), and Normalized Differential Salinity Index (NDSI), the study meticulously delineated playa boundaries, shedding light on their geographic distribution, economic potential, and environmental significance.

The findings underscored the efficacy of AWEI and NDSI in accurately extracting water bodies and identifying saline areas within playas, as evidenced by their high overall accuracy and kappa coefficient values.

Furthermore, the validation process, utilizing ground truth data, reinforced the reliability of the delineated boundaries, enhancing the study's credibility and ensuring a comprehensive understanding of playa dynamics in the region.

The geographic distribution analysis showed that playas are dispersed across various counties in Isfahan province, with notable concentrations in Isfahan and Nain counties. These playas, characterized by their vast expanses and unique geological features, harbour significant economic potential yet remain relatively underutilized.

One standout feature among the identified playas is the Gavkhuni Playa, renowned as the largest salt playa in Isfahan province. Situated at the entrance of the Varzaneh Desert, its ecological significance has been marred by declining water inflows from the Zayandeh Rud River, resulting in environmental degradation and biodiversity loss.

ACKNOWLEDGMENT. I would like to express my sincere appreciation to the Isfahan Regional Water Organization for their invaluable support in funding and supervising this research project.

References

Acharya, T. D., Yang, I. (2015): Exploring Landsat 8, International Journal of IT, Engineering and Applied Sciences Research (IJIEASR), 4 (4), 4–10.

Adam, E., Mutanga, O., Rugege, D. (2010): Multispectral and hyperspectral remote sensing for identification and mapping of wetland vegetation: a review, Wetlands Ecology and Management, 18 (3), 281–296.

Bowen, M. W., Johnson, W. C., Egbert, S. L., Klopfenstein, S. T. (2010): A GIS-based Approach to Identify and Map Playa Wetlands on the High Plains, Kansas, USA, Wetlands, 30 (4), 675–684.

Dixon, L. F. J. (1998): Analytical photogrammetry for geomorphological research, Landform monitoring modeling and analysis.

Embabi, N. S., Moawad, M. B. (2014): A semi-automated approach for mapping geomorphology of El Bardawil Lake, Northern Sinai, Egypt, using integrated remote sensing and GIS techniques, The Egyptian Journal of Remote Sensing and Space Science, 17 (1), 41–60.

Feyisa, G. L., Meilby, H., Fensholt, R., Proud, S. R. (2014): Automated Water Extraction Index: A new technique for surface water mapping using Landsat imagery, Remote Sensing of Environment, 140, 23–35.

Gao, B.-c. (1996): NDWI – A normalized difference water index for remote sensing of vegetation liquid water from space, Remote Sensing of Environment, 58 (3), 257–266.

Gasmi, A., Gomez, C., Chehbouni, A., Dhiba, D., Elfil, H. (2022): Satellite Multi-Sensor Data Fusion for Soil Clay Mapping Based on the Spectral Index and Spectral Bands Approaches, Remote Sensing, 14, 1103.

Guo, Q., Pu, R., Li, J., Cheng, J. A. (2017): Weighted normalized difference water index for water extraction using Landsat imagery, International Journal of Remote Sensing, 38, 5430–5445.

Halabisky, M., Miller, D., Stewart, A. J., Lorigan, D., Brasel, T., Moskal, L. M. (2022): The Wetland Intrinsic Potential tool: Mapping wetland intrinsic potential through machine learning of multi-scale remote sensing proxies of wetland indicators, EGUsphere, 1–19.

Hammond, E. H. (1964): Analysis of properties in land form geography: An application to broad-scale land form mapping, Annals of the American Association of Geographers, 54, 11–19.

Haukos, D. A., Smith, L. M. (1994): The importance of playa wetlands to biodiversity of the Southern High Plains, Landscape and Urban Planning, 28 (1), 83–98.

Kaplan, G., Avdan, U. (2017): Mapping and monitoring wetlands using Sentinel-2 satellite imagery, ISPRS Ann. Photogramm. Remote Sens, Spatial Inf. Sci., IV-4/W4, 271–277.

Khan, N. M. (2002): Analysis of environmental land degradation caused by hydro-salinity in semi-arid irrigated regions.

Khan, N. M., Sato, Y. (2001): Monitoring hydro-salinity status and its impact in irrigated semi-arid areas using IRS-1B LISS-II data, Asian J. Geoinform, 1 (3), 63–73.

Lang, M., Bourgeau-Chavez, L., Tiner, R., Klemas, V. (2015): Advances in Remotely Sensed Data and Techniques for Wetland Mapping and Monitoring, 79–116.

Loveland, T. R., Irons, J. R. (2016): Landsat 8: The plans, the reality, and the legacy, Remote Sensing of Environment, 185, 1–6.

Lyon, J. G., Lopez, R. D., Lyon, L. K., Lopez, D. (2001): Wetland Landscape Characterization: GIS, Remote Sensing and Image Analysis.

Miller, H. M. (2016): Users and uses of Landsat 8 satellite imagery – 2014 survey results (2016-1032), Retrieved from Reston, VA: http://pubs.er.usgs.gov/publication/ofr20161032.

Mirzadeh, S. M., Jin, S., Amani, M. (2023): Spatial-Temporal Changes of Abarkuh Playa Landform from Sentinel-1 Time Series Data, Remote Sensing, 15 (11).

Mitsch, W. J., Gosselink, J. G., Zhang, L., Anderson, C. J. (2009): Wetland Ecosystems: Wiley.

Mui, A., He, Y., Weng, Q. (2015): An object-based approach to delineate wetlands across landscapes of varied disturbance with high spatial resolution satellite imagery, ISPRS Journal of Photogrammetry and Remote Sensing, 109, 30–46.

Ozesmi, S. L., Bauer, M. E. (2002): Satellite remote sensing of wetlands, Wetlands Ecology and Management, 10 (5), 381–402.

Rebelo, L.-M., Finlayson, M., Nagabhatla, N. (2008): Remote Sensing and GIS for Wetland Inventory, Mapping and Change Analysis, Journal of environmental management, 90, 2144–2153.

Sader, S. A., Ahl, D., Liou, W.-S. (1995): Accuracy of Landsat-TM and GIS rule-based methods for forest wetland classification in Maine, Remote Sensing of Environment, 53 (3), 133–144.

Schneevoigt, N. J., Schrott, L. (2006): Linking geomorphic systems theory and remote sensing: a conceptual approach to Alpine landform detection (Reintal, Bavarian Alps, Germany), Geogr. Helv., 61 (3).

Smith, M. J., Paron, P., Griffiths, J. S. (2011): Chapter Eight – Digital Mapping: Visualisation, Interpretation and Quantification of Landforms, Developments in Earth Surface Processes, Elsevier, 15, 225–251.

Slaymaker, O. (2001): The role of remote sensing in geomorphology and terrain analysis in the Canadian Cordillera, The International Journal of Applied Earth Observation, 3, 11–17.

Tulbure, M. G., Broich, M., Stehman, S. V., Kommareddy, A. (2016): Surface water extent dynamics from three decades of seasonally continuous Landsat time series at subcontinental scale in a semi-arid region, Remote Sensing of Environment, 178, 142–157.

Wu, Q. (2018): GIS and Remote Sensing Applications in Wetland Mapping and Monitoring conference.

Xu, H. (2006): Modification of normalized difference water index (NDWI) to enhance open water features in remotely sensed imagery, International Journal of Remote Sensing, 27, 3025–3033.

Xu, X., Xu, S., Jin, L., Song, E. (2011): Characteristic analysis of Otsu threshold and its applications, Pattern Recognit. Lett, 32, 956–961.

URL

URL 1: USGS Science for a Changing World, https://www.usgs.gov/faqs/what-are-band-designations-landsat-satellites, (2.1.2024).

Istraživanje obrazaca suhih jezerskih korita u Pokrajini Isfahan primjenom tehnologije daljinskih istraživanja

SAŽETAK. Suha jezerska korita ključna su područja za skladištenje i napajanje vodom u pretežno suhoj i polusuhoj klimi. Kartiranje suhih jezerskih korita pomaže u određivanju njihove lokacije, veličine i hidroloških značajki te pruža vrijedne informacije za procjenu dostupnosti vode, planiranje održive upotrebe vode i razumijevanje uloge suhih jezerskih korita u obnavljanju podzemne vode. Pošto nije bilo provedeno sveobuhvatno istraživanje u smislu identificiranja svih suhih jezerskih korita u Pokrajini Isfahan, utvrđivanje odgovarajuće metode za njihovo otkrivanje može biti značajan korak u razumijevanju, upotrebi i očuvanju takvih područja. Primjena daljinskih istraživanja kao učinkovitog, brzog i vrlo preciznog rješenja može učinkovito identificirati ove pojave. U tom smislu prikupljene su satelitske snimke Landsat koje obuhvaćaju različite mjesece tijekom 2023. godine za Pokrajinu Isfahan. Integracija različitih spektralnih indeksa, kao što su NDWI, SWI i AWEI za detekciju vode i NDSI za slana područja, značajno povećava preciznost prostornog ograničavanja suhih jezerskih korita. Nakon primjene filtara i spektralnih indeksa na satelitske slike Landsat, identificirana su ukupno 24 suha jezerska korita unutar Pokrajine Isfahan. Značajno je da su okruzi Isfahan i Nain imali najveći broj suhih jezerskih korita, odnosno devet i sedam pojedinačno. Među utvrđenim suhim jezerskim koritima najznačajnija je površina zabilježena u Khuru koja pokriva približno 2250 kvadratnih kilometara sa značajnim dijelom površine pokrivenom slanom korom koja doseže do 1300 kvadratnih kilometara. Kako bi se potvrdila točnost rezultata, proveden je precizan postupak koji je uključivao prikupljanje 106 stvarnih točaka na tlu primjenom GPS mjerenja. Ta procjena potvrđuje točnost iscrtavanja granica, naglašavajući učinkovitost daljinskih istraživanja i GIS tehnologije u tom kontekstu.

Ključne riječi: sušna područja, Geografski informacijski sustav (GIS), Pokrajina Isfahan, kartiranje suhih jezerskih korita, daljinska istraživanja, spektralni indeksi.

Received / Primljeno: 2024-01-05

Accepted / Prihvaćeno: 2024-03-20